


# Analysis of Differences in Electrochemical Performance Between Coin and Pouch Cells for Lithium-Ion Battery Applications

Yeonguk Son, Hyungyeon Cha, Taeyong Lee, Yujin Kim, Adam Boies, Jaephil Cho\*, and Michael De Volder\* 

Small coin cell batteries are predominantly used for testing lithium-ion batteries (LIBs) in academia because they require small amounts of material and are easy to assemble. However, insufficient attention is given to difference in cell performance that arises from the differences in format between coin cells used by academic researchers and pouch or cylindrical cells which are used in industry. In this article, we compare coin cells and pouch cells of different size with exactly the same electrode materials, electrolyte, and electrochemical conditions. We show the battery impedance changes substantially depending on the cell format using techniques including Electrochemical Impedance Spectroscopy (EIS) and Galvanostatic Intermittent Titration Technique (GITT). Using full cell NCA-graphite LIBs, we demonstrate that this difference in impedance has important knock-on effects on the battery rate performance due to ohmic polarization and the battery life time due to Li metal plating on the anode. We hope this work will help researchers getting a better idea of how small coin cell formats impact the cell performance and help predicting improvements that can be achieved by implementing larger cell formats.

## 1. Introduction

Research on lithium-ion batteries (LIBs) has expanded tremendously over the past decade, because they are one of the most promising battery technologies for both electric cars and portable electronic devices.<sup>[1–5]</sup> Despite this intensification of research activities, most academic works is focusing on coin cells because larger format pouch and cylindrical cells require more active material as well as expensive

infrastructure (e.g., roll-to-roll coaters, dry rooms, cell stackers). The assumption in most papers is that the battery performance is independent of the cell format. While this is true for some metrics, such as the gravimetric capacity, we show in this article that, for instance, the cycling stability and rate performance are influenced by the cell format (even if all coating parameters such as the areal loading, calendaring are the same).

Different battery cell types and sizes have been meaningfully investigated in the several reports.<sup>[6–10]</sup> For instance, evolved gas can be accommodated more easily in coin cells due to their large volume compared with the electrode area, and the electrical impedance of different cell types is known to be different. However, variations in the impedance properties of different cell types still remain ambiguous. Ultimately, a good understanding of differences in coin cell versus pouch cell performance is important to predict how lab scale measurements on small coin cells trans-


late to industrially relevant pouch cell performance. Herein, we investigate the differences between coin cells (capacity ~7 mAh) and pouch type cells (capacity of 24, 350, 750, and 1000 mAh). We observed differences in cell impedance by using various electrochemical techniques such as Electrochemical Impedance Spectroscopy (EIS), Galvanostatic Intermittent Titration Technique (GITT), Direct Current Internal Resistance (DC-IR), and a new electrochemical current pulse method. We then show how cell impedance influences the capacity retention during cycling and rate performance. These results are useful to close the gap between university laboratory and industrial cell results.

## 2. Results and Discussion

As depicted in **Figure 1a**, pouch cells are composed of a cathode, separator, and anode in either a single layer or multiple layer stack (usually with double side coated electrodes) that are encapsulated in a pouch. By comparison, coin cells count more components. As shown in **Figure 1a**, they comprise a can, anode, separator, gasket, cathode, spacer, spring, and cap. In our experiments, we use a  $\text{LiNi}_{0.88}\text{Co}_{0.1}\text{Al}_{0.02}\text{O}_2$  (NCA) cathode and graphite anode. To further

Prof. Y. Son, Prof. A. Boies, Prof. M. De Volder  
Department of Engineering, University of Cambridge, 17 Charles Babbage Road, CB3 0FS, Cambridge UK  
E-mail: [mfd2@cam.ac.uk](mailto:mfd2@cam.ac.uk)

Prof. Y. Son  
Department of Chemical Engineering, Changwon National University, Changwon Gyeongsangnam-do 51140, Korea  
Dr. H. Cha, Dr. T. Lee, Y. Kim, Prof. J. Cho  
Department of Energy Engineering, School of Energy and Chemical Engineering, Ulsan National Institute of Science and Technology (UNIST), Ulsan 44919, Korea  
E-mail: [jpcho@unist.ac.kr](mailto:jpcho@unist.ac.kr)

 The ORCID identification number(s) for the author(s) of this article can be found under <https://doi.org/10.1002/eeem2.12615>.

DOI: 10.1002/eeem2.12615

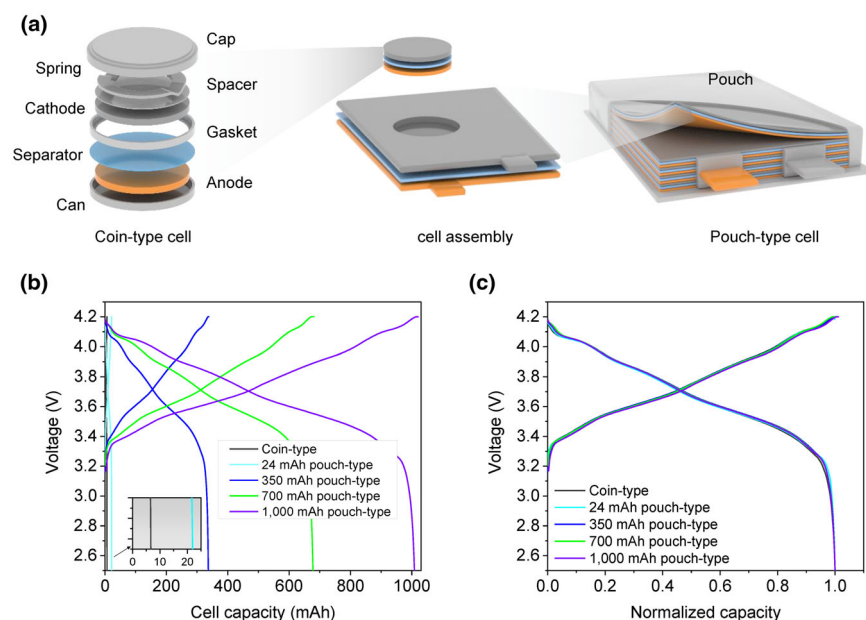


**Figure 1.** Schematic and electrochemical characterization of coin-type and pouch-type cell. a) Schematics of coin-type cell and pouch-type cell. b) Voltage profiles and c) Normalized voltage profiles of 7 mAh coin-type cell, 24, 350, 700, and 1000 mAh pouch-type cells for the 2nd cycle.

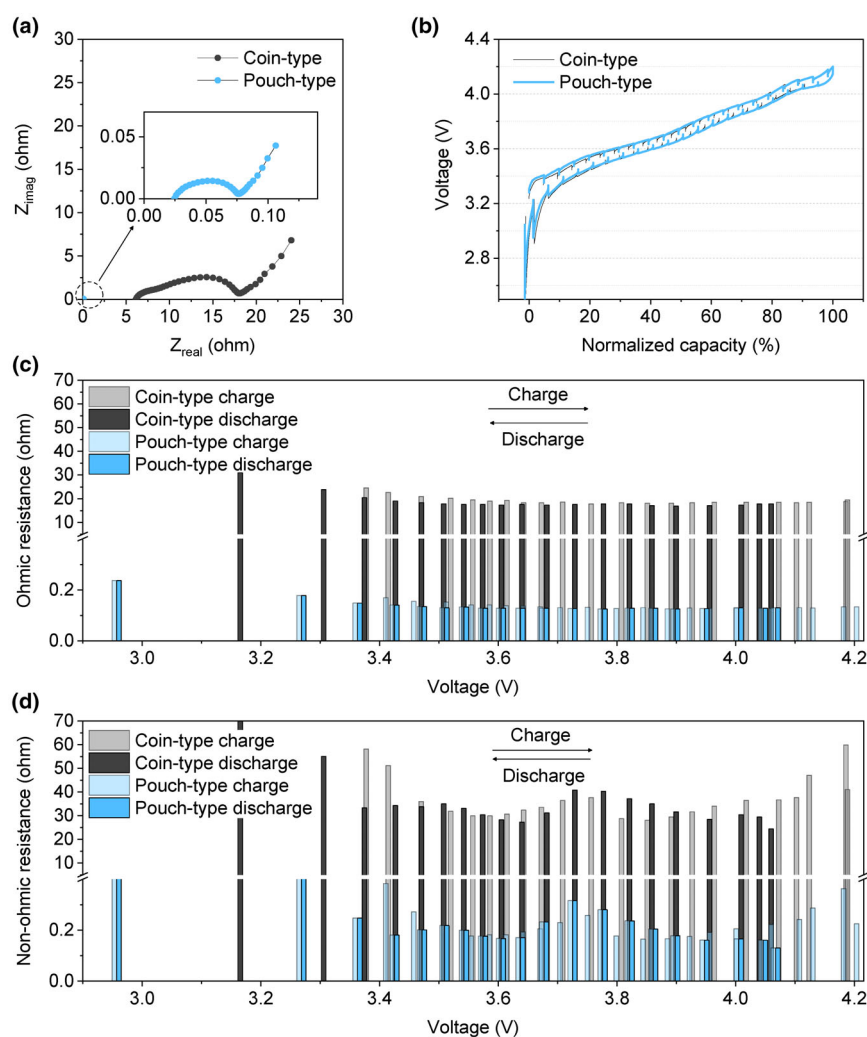
ensure that our experiments are representative of practical commercial batteries, high areal loading levels of  $22.8 \text{ mg cm}^{-2}$  on the cathode and  $13.1 \text{ mg cm}^{-2}$  on the anode were used, respectively, and the N/P ratio was 1.1.<sup>[11,12]</sup> The cathode and anode were calendared to densities of 3.0 and  $1.6 \text{ g cm}^{-3}$ , respectively. The same electrodes are used in our coin and pouch cell experiments. The only difference is that one-side-coated electrodes are used for coin cells and double-side-coated electrodes are used for pouch cells. The coin cell cathode has a diameter of 14 mm and the anode has a 16 mm diameter. Pouch cells of 24, 350, 700, and 1000 mAh are fabricated and tested. The 24 mAh cells are made with small electrodes of 20 mm by 25 mm and the larger format cell are using cathodes of 50.0 mm by 68.5 mm. The size of the anodes is slightly larger (54.0 mm by 72.5 mm) to avoid dendrite growth.<sup>[13,14]</sup> Our 350 mAh cells use only 1 cathode and 2 anodes (2 pairs), 700 mAh cells use 2 cathodes and 3 anodes (4 pairs), whereas 3 cathodes and 4 anodes are used for 1000 mAh cells (6 pairs). We assembled multiple cells (at least three cells) of each type, and as shown in Figure S1, Supporting Information, there is very little cell to cell variation in our experiments. The details of the electrode preparation are described in the experimental procedure. All the cells are cycled between 2.5 and 4.2 V in triplicates at 25 °C using a WonAtech battery cyler.

Figure S2, Supporting Information, shows the formation voltage profiles of the coin and pouch cells. The initial coulombic efficiency of coin and pouch cells are 86.3% and 86.2%, respectively, which is within the margin of error of the measurements. However, the pouch cells repeatedly show a lower voltage profile in the first charging process than coin cell. Note that the kink in charge profile of the pouch cell is derived from degassing step, which is essential for large pouch cells (details are provided in the experimental procedure). In contrast, discharging profiles and subsequent cycles in coin and 24, 350, and 700 mAh pouch cells coincide completely for all the different cell formats as shown in Figure 1b,c.

To investigate the internal resistance difference induced by different cell type, we conducted various electrochemical analysis methods, such as EIS, GITT, DC-IR, and a modified DC-IR technique (see details in the experimental procedure). Figure 2a shows the resistance analysis using EIS with 7 mAh coin-type cell and 1000 mAh pouch-type cell. The high frequency series resistances of coin and pouch cells are 6.227 and 0.025 ohm, respectively. The combined semi-circles length, representing resistances resulting from the solid electrolyte interphase (SEI), and charge transfer of coin and pouch cells are 11.84 and 0.05 ohm, respectively. This is a surprisingly large difference of over 200 fold. To verify this result, we also use GITT to analyze the resistance differences between the coin and pouch cells. Figure 2b shows raw GITT data of coin and pouch cells (after two formation cycles at 0.1 C), which illustrates that the open circuit voltage of the coin cell and pouch cells stabilize to the same values as expected. However, ohmic resistances of the coin and pouch cells derived from GITT are very different as shown in Figure 2c as a function of the cell voltage. The

ohmic resistances of coin and pouch cells are around 19 and 0.14 ohm on average, respectively. The ohmic resistances are similar during charge and discharge as expected. The nonohmic resistances of coin cells vary from 24 to 176 ohm and pouch cells from 0.13 to 5.23 ohm as a function of the state of charge and charging and discharging (Figure S3, Supporting Information, illustrates how we derive ohmic and nonohmic voltage drop contributions<sup>[15,16]</sup>). To further confirm this large difference in impedance between coin and pouch cells, we carried out DC-IR tests (Figure S4, Supporting Information), by applying current pulses of various sizes at the same SOC (here 60%).<sup>[17]</sup> We found that for a coin cell, the ohmic resistance is 11.424 ohm and for a pouch cell it is 0.056 ohm.

To further study these trends in impedance for the 24, 350, and 700 mAh cells discussed above, DC-IR measurement was conducted with each cell. Figure 3a shows the DC-IR resistance at 60% SOC for all these difference cell sizes. The DC-IR resistance of the cells is decreasing as the cell size is increasing. Figure 3b scheme explains the reason of this trend. Increasing the cell size means effectively that more LIBs are connected in parallel.<sup>[18,19]</sup> In essence, this is analogous to connecting resistors in parallel where the total resistance of  $N$  resistors in parallel is  $R/N$ . In the case of batteries,  $N$  is proportional to the electrode area, and therefore, if we multiply the impedance by the cell area, a normalized resistance is obtained that is almost independent of the cell format. Normalizing impedance per geometric area (i.e., current collector surface) allows for comparison between batteries using the same electrode formulation, but is not taking into account the areal loading, which makes comparison between different electrodes challenging, and therefore, we suggest to normalize impedance per cell capacity in this study: in this case 108, 85, 85, 81, and 76 ohm mAh for 7, 22, 337, 678, and 1008 mAh cells, respectively (Figure 3a). The slightly higher normalized coin cell resistance is probably due to additional contact resistances introduced by the springs and spacers used in coin cells. However, this calculation allows to directly predict the impedance of



**Figure 2.** Internal resistance measured by electrochemical tests. a) EIS and b) GITT results for the coin-type and pouch-type cell. c) Ohmic resistance and d) nonohmic resistance calculated by each pulse from GITT measurement in Figure 2b.

large format cells simply based on the electrode areas or the cell capacity.

While the ohmic resistance does not change with the current density, nonohmic resistance may change with the current density, which has not been studied in detail so far. In this study, we suggest a modified DC-IR method where pulses with the same total charge are applied but with a varying current density and time. Instead of applying different current densities for the same time, we suggest, for instance, to apply a current rate of 0.5 C/−0.5 C for 100 s, 1 C/−1 C for 50 s, 2 C/−2 C for 25 s, 3 C/−3 C for 16.7 s, 4 C/−4 C for 12.5 s, 5 C/−5 C for 10 s, and 10 min rest in between each step (see details in the experimental procedure, Figure S5, Supporting Information). In other words, instead of applying current for a constant time (10 s), we suggest keeping the applied charge in each pulse constant. Although the ohmic voltage drops in both DC-IR methods are almost same, the non-ohmic voltage drops of the modified DC-IR are significantly different (Figure S6a,b, Supporting Information). Note that the comparison of conventional and modified DC-IR methods shown in Figure 4 is based on the 1 Ah pouch cells. The trend of comparison is same in the coin

cells (Figure S7, Supporting Information). If the voltage drops are converted to resistance, the ohmic resistances of the results from the DC-IR and modified DC-IR remain almost the same. However, the nonohmic resistance from the modified DC-IR is significantly different depending on C-rate (Figures S6 and S7, Supporting Information). In other words, if the same amount of charge applied per pulse is constant, the nonohmic resistance value increases as the C-rate decreases.

The difference in impedance observed as a function of the cell format has important knock-on effects on the electrochemical performance of the batteries. As shown in Figure 4a, the rate performance observed in pouch cells is better than coin cells despite using the exact same electrodes due to ohmic polarization. Further, as shown in Figure 4b, we observed a faster capacity fade in coin cells than pouch cells. Considering that we used exactly identical electrodes and electrolyte, this difference also originates from the internal resistance in different cell configurations. More specifically, the effective cut-off voltages observed by the active materials shift with the cell impedance, leading to harsher effective voltages in coin cells than pouch cells. To quantify this, EIS analysis is carried out after 100 cycles and 500 cycles showing a noticeable increase (43%) in impedance after 100 cycles in coin cell, whereas pouch cell shows only slight increase (10%) in impedance (Figure 4c,d). In other words, the initial higher impedance of coin cells can lead to faster degradation of the electrode, which in turn leads to more impedance build-up in the cells as cycling goes on. After 500 cycles, both coin and pouch cells show a substantial increase in impedance.

Figure 4c shows a faster decrease in capacity in coin cells, which is particularly apparent in the first 100 cycles. To verify this, we carried out postmortem SEM measurement of the anodes (Figure 4e,f) and cathodes (Figure S8, Supporting Information) after 100 and 500 cycles. The coin cell anodes showed minor signs of Li plating after 100 cycles and substantial plating after 500 cycles (yellow regions in Figure 4e). In contrast, the anodes in pouch cells show a very clean surface even after 500 cycles. This capacity loss is in line with the above postmortem SEM observations and impedance and is probably due to a number of mechanisms, including the decrease in lithium inventory due to the side reactions observed on the anode.<sup>[20–22]</sup>

### 3. Conclusions

Academic advances in LIBs research are typically carried out using coin cells. The underlying assumption in these reports is that the results observed in coin cells also hold true for larger format cells

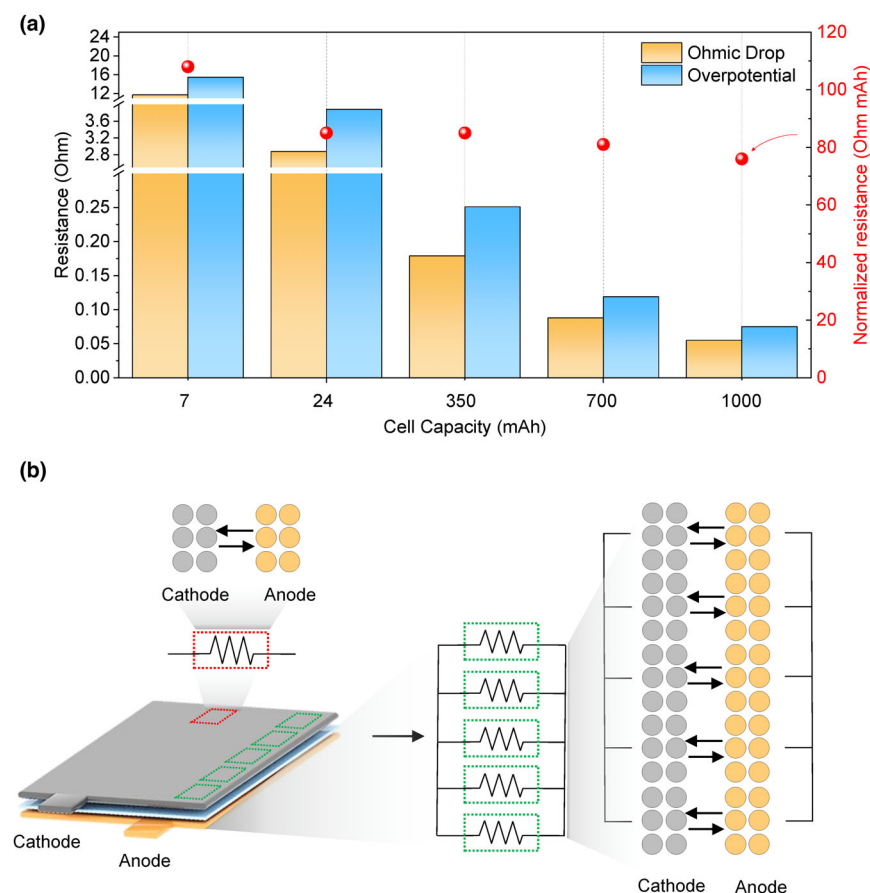


**Figure 3.** Calculation of resistance from various cell. a) Resistance and normalized resistance calculated from DC-IR results with 7, 24, 350, 700, and 1000 mAh cell. b) Schematics explaining resistance term with parallel reaction concept.

used in commercial applications. While this is true for certain metrics such as the specific capacity, this article shows how the cell format can influence properties such as rate performance and cycling stability, even if the cells are using the exact same cathode (NCA) and anode (graphite) materials and electrode-coating parameters. The main cause for these differences lies in the cell impedance, which is more than 100 times higher in coin cells (~7 mAh) than in pouch cells (~1 Ah). This is explained by an equivalent electrical circuit with 24 to 350, 700, and 1000 mAh pouch cells and coin cells, which can be used to predict the impedance of cells as they are scaled up. As expected, the lower impedance in pouch cells results in a better rate performance. We also observed that the higher resistance coin cells are more likely to have undesirable side reactions such as Li plating during the cycling and therefore show a lower capacity retention. Overall, these observations help predicting how properties observed coin cells can change when transitioning to larger commercial pouch cell formats.

## 4. Experimental

**Electrode preparation:** The commercial NCA cathode sample was mixed with polyvinylidene fluoride (PVDF) binder and super-P carbon with a mass ratio of 94:3:3 in N-Methyl-2-pyrrolidone (NMP) solvent. The commercial natural graphite

anode sample was mixed with carboxymethyl cellulose (CMC)/styrene-butadiene rubber (SBR) binder and super-P with a mass ratio of 97.5:1:1.5 in deionized water solvent. Amounts of slurry batch for the cathode and anode were prepared over 1 kg and 500 g, respectively, for large scale roll to roll electrode processing up to 30 m. The loading levels of cathode and anode were 22.8 and 13.1 mg cm<sup>-2</sup>, respectively. After roll-to-roll electrode processing, the electrodes were pressed to increase the electrode density up to 3.0 g cm<sup>-3</sup> (for cathode) and 1.6 g cm<sup>-3</sup> (for anode). Finally, the electrodes were vacuum-dried at 120 °C over 6 h, just before the cell assembly.

**Coin cell assembly:** 2032-type coin cells were used for the coin cell tests. The assembly was conducted in the glove box. The sizes of cathode and anode are 14 and 16 mm diameters, respectively. To avoid mismatch of cathode and anode, the assembly was very carefully conducted by the skilled researcher. The electrolyte of 1.15 M LiPF<sub>6</sub> in mixture of ethylene carbonate/ethyl methyl carbonate/diethyl carbonate (3/6/1 by volume) with 10% fluoroethylene carbonate (Panax Starlyte) was used. Microporous polyethylene separator (15 μm, Celgard) was used.

**Pouch cell assembly:** 22, 337, 678, and 1008 mAh full cells were fabricated in the dry room. In terms of 22 mAh full cell, the areas of cathode and anode are 5 and 5.94 cm<sup>2</sup> and those of other cells are 34.2 and 39.2 cm<sup>2</sup>. The anode and cathode were carefully stacked and stacking number of the 337, 678, and 1008 mAh is 1, 2, and 3, respectively. The electrolyte of 1.15 M LiPF<sub>6</sub> in mixture of ethylene carbonate/ethyl methyl carbonate/diethyl carbonate (3/6/1 by volume) with 10% fluoroethylene carbonate (Panax Starlyte) was used. We injected sufficient amounts of electrolyte in the cells to prevent the performance to be affected by electrolyte starvation. The amount of electrolyte used for 1 Ah, 678, 337, and 22 mAh cells was 4 g, 2.6 g, 1.3 g and 100 μL, respectively. In the case of coin cells, roughly 0.5 g of electrolyte was

used, but it is important to note that during the cell assembly process, excess electrolyte can flow out of the cells.<sup>[23,24]</sup> Microporous polyethylene separator (15 μm, Celgard) was used. Assembled cells were aged for 24 h and charged to SOC 30% with a 0.1 C-rate, followed by degassing step. After degassing process, formation cycles were performed with a 0.1 C rate in a voltage range of 2.5–4.2 V.

**Battery performance:** Cut-off voltage of 4.3 V and constant voltage cut-off of 0.05 C were conducted in charging process of all cell tests. Cut-off voltage of 2.5 V was conducted in discharging process of all cell tests. For the formation 2 cycles, the 0.1 C was used in both charging and discharging. For the cycling test, 0.5 C charging and 1 C discharging were used up to 500 cycles. For the rate test of each 5 cycles, 0.5 C charging rate was fixed and discharging rate range of 0.5, 1, 2, 3, 4, and 5 C was used. To avoid the errors from remained lithium ion at high rate test, the cells were fully re-discharged at 0.5 C for each cycle.

**EIS:** The EIS measurement was conducted with frequency range from 1000 kHz to 10 mHz and amplitude of 10 mV. All the measurements were conducted at fully charged state.

**GITT:** Cut-off voltage of 4.3–2.5 V was conducted in GITT test. The pulse current was 0.1 C for 30 min, followed by 2 h rest time.

**DC-IR:** DC-IR applied pulse current for every 20% SOC changes. The applied current and time are 0.5 C/–0.5 C for 10 s, 1 C/–1 C for 10 s, 2 C/–2 C for 10 s, 3 C/–3 C for 10 s, 4 C/–4 C for 10 s, 5 C/–5 C for 10 s, and 10 min rest whenever changing the current.

**Modified DC-IR:** Modified DC-IR applied pulse current for every 20% SOC changes. the applied current and time are 0.5 C/–0.5 C for 100 s, 1 C/–1 C for 50 s, 2 C/–2 C for 25 s, 3 C/–3 C for 16.7 s, 4 C/–4 C for 12.5 s, 5 C/–5 C for 10 s, and 10 min rest whenever changing the current.



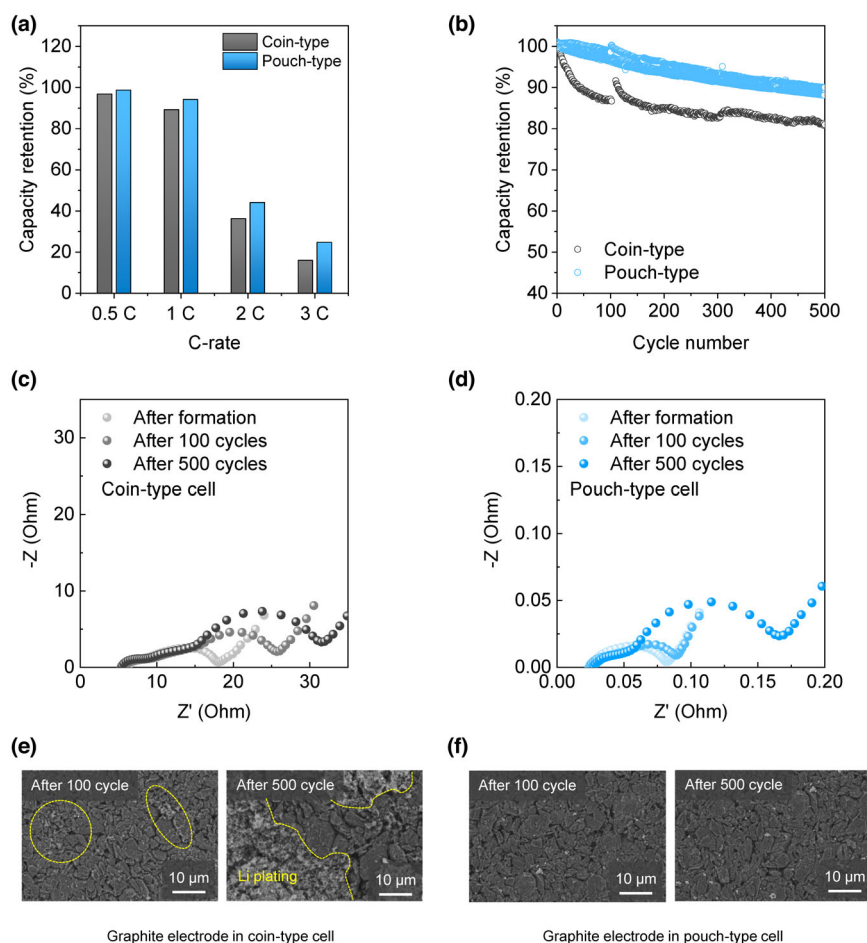


**Figure 4.** Electrochemical performance and microstructure change of graphite anode after cycling. a) Rate performance and b) cycle performance of coin-type and pouch-type cell voltage ranged from 2.5 to 4.2 V. EIS results after formation, 100 cycles, and 500 cycles for the c) coin-type cell and d) pouch-type cell. SEM results of graphite anode after 100 cycles and 500 cycles for e) coin-type cell and f) pouch-type cell.

*Ex situ SEM:* The morphological change of the electrode samples was observed using scanning electron microscopy (SEM, VERIOS 460, FEI).

## Acknowledgements

Y.S. and H.C. contributed equally to this work. We acknowledge funding from the ERC (Consolidator Grant MIGHTY, 866005), the Innovate UK (UKRI: 104174), and Faraday Institution - Future CAT (FIRG017) and Degradation (FIRG001).

The table of contents entry should be 50–60 words long and should be written in the present tense. The text should be different from the abstract text.

Academic advances in lithium-ion battery research are typically carried out using coin cells. However, the applying to the larger cell format could bring unexpected implications on the cell life time and cycling stability. In this work, we present a new perspective on how scaling-up academic research to commercial cell formats can lead to differences in battery performance.

## Conflict of Interest

The authors declare no conflict of interest.

## Supporting Information

Supporting Information is available from the Wiley Online Library or from the author.

## Keywords

coin cell, full cell, lithium-ion batteries, pouch cell

Received: November 30, 2022

Revised: February 22, 2023

Published online: March 1, 2023

- [1] J. M. Tarascon, M. Armand, *Nature* **2001**, 414, 359.
- [2] Z. P. Cano, D. Banham, S. Ye, A. Hintennach, J. Lu, M. Fowler, Z. Chen, *Nat. Energy* **2018**, 3, 279.
- [3] X. Zeng, M. Li, D. Abd El-Hady, W. Alshitari, A. S. Al-Bogami, J. Lu, K. Amine, *Adv. Energy Mater.* **2019**, 9, 1900161.
- [4] R. Schmich, R. Wagner, G. Hörpel, T. Placke, M. Winter, *Nat. Energy* **2018**, 3, 267.
- [5] S. Chen, F. Dai, M. Cai, *ACS Energy Lett.* **2020**, 5, 3140.
- [6] S. Chen, C. Niu, H. Lee, Q. Li, L. Yu, W. Xu, J.-G. Zhang, E. J. Dufek, M. S. Whittingham, S. Meng, J. Xiao, J. Liu, *Joule* **2019**, 3, 1094.
- [7] Y. Son, H. Cha, C. Jo, A. S. Groombridge, T. Lee, A. Boies, J. Cho, M. De Volder, *Mater. Today Energy* **2021**, 21, 100838.
- [8] M. Hagen, D. Hanselmann, K. Ahlbrecht, R. Maça, D. Gerber, J. Tübke, *Adv. Energy Mater.* **2015**, 5, 1401986.
- [9] S. Dörfler, H. Althues, P. Härtel, T. Abendroth, B. Schumm, S. Kaskel, *Joule* **2020**, 4, 539.
- [10] X.-B. Cheng, C. Yan, J.-Q. Huang, P. Li, L. Zhu, L. Zhao, Y. Zhang, W. Zhu, S.-T. Yang, Q. Zhang, *Energy Stor. Mater.* **2017**, 6, 18.
- [11] Y. Cao, M. Li, J. Lu, J. Liu, K. Amine, *Nat. Nanotechnol.* **2019**, 14, 200.
- [12] Z. Lin, T. Liu, X. Ai, C. Liang, *Nat. Commun.* **2018**, 9, 5262.
- [13] V. Murray, D. S. Hall, J. R. Dahn, *J. Electrochem. Soc.* **2019**, 166, A329.
- [14] J. Hu, B. Wu, S. Chae, J. Lochala, Y. Bi, J. Xiao, *Joule* **2021**, 5, 1011.
- [15] W. Weppner, R. A. Huggins, *J. Electrochem. Soc.* **1977**, 124, 1569.
- [16] Y. Son, T. Lee, B. Wen, J. Ma, C. Jo, Y.-G. Cho, A. Boies, J. Cho, M. De Volder, *Energy Environ. Sci.* **2020**, 13, 3723.
- [17] K. Jong Hoon, L. Seong Jun, L. Jae Moon, C. Bo Hyung, Presented at 2007 7th International Conference on Power Electronics, 22–26 Oct. 2007.
- [18] J. Billaud, F. Bouville, T. Magrini, C. Villevieille, A. R. Studart, *Nat. Energy* **2016**, 1, 16097.
- [19] M. Ebner, D.-W. Chung, R. E. García, V. Wood, *Adv. Energy Mater.* **2014**, 4, 1301278.
- [20] C. Uhlmann, J. Illig, M. Ender, R. Schuster, E. Ivers-Tiffée, *J. Power Sources* **2015**, 279, 428.
- [21] F. Ringbeck, C. Rahe, G. Fuchs, D. U. Sauer, *J. Electrochem. Soc.* **2020**, 167, 90536.
- [22] W. M. Dose, C. Xu, C. P. Grey, M. De Volder, *Cell Rep. Phys. Sci.* **2020**, 1, 100253.
- [23] S. J. An, J. Li, C. Daniel, H. M. Meyer, S. E. Trask, B. J. Polzin, D. L. Wood III, *ACS Appl. Mater. Interfaces* **2017**, 9, 18799.
- [24] S. J. An, J. Li, D. Mohanty, C. Daniel, B. J. Polzin, J. R. Croy, S. E. Trask, D. L. Wood III, *J. Electrochem. Soc.* **2017**, 164, A1195.